

Article

Composition, Structure, and Properties of Ti, Al, Cr, N, C Multilayer Coatings on AISI W1-7 Alloyed Tool Steel

Tetiana Loskutova ¹, Michal Hatala ², Inna Pogrebova ³, Natalya Nikitina ⁴, Maryna Bobina ¹, Svetlana Radchenko ^{2,*} , Nadiia Kharchenko ⁵, Serhii Kotlyar ¹, Ivan Pavlenko ⁶  and Vitalii Ivanov ⁷ 

¹ Department of Physical Materials Science and Heat Treatment, Y.O. Paton Institute of Materials Science and Welding, National Technical University of Ukraine “Igor Sikorsky Kyiv Polytechnic Institute”, 37, Peremohy Ave., 03056 Kyiv, Ukraine; losktv@ukr.net (T.L.); bobinamn@ukr.net (M.B.); s.kotlyar@kpi.ua (S.K.)

² Department of Automobile and Manufacturing Technologies, Faculty of Manufacturing Technologies, Technical University of Kosice, 1, Bayerova St., 080 01 Presov, Slovakia; michal.hatala@tuke.sk

³ Department of Electrochemical Productions Technology, Faculty of Chemical Technology, National Technical University of Ukraine “Igor Sikorsky Kyiv Polytechnic Institute”, 37, Peremohy Ave., 03056 Kyiv, Ukraine; i.pogrebova@kpi.ua

⁴ Department of English for Engineering 2, Faculty of Linguistics, National Technical University of Ukraine “Igor Sikorsky Kyiv Polytechnic Institute”, 37, Peremohy Ave., 03056 Kyiv, Ukraine; n.nikitina@kpi.ua

⁵ Department of Applied Materials Science and Technology of Structural Materials, Faculty of Technical Systems and Energy Efficient Technologies, Sumy State University, 2, Rymaskogo-Korsakova St., 40007 Sumy, Ukraine; n.harchenko@pmtkm.sumdu.edu.ua

⁶ Department of Computational Mechanics—Volodymyr Martynovskyy, Faculty of Technical Systems and Energy Efficient Technologies, Sumy State University, 2, Rymaskogo-Korsakova St., 40007 Sumy, Ukraine; i.pavlenko@omdm.sumdu.edu.ua

⁷ Department of Manufacturing Engineering, Machines and Tools, Faculty of Technical Systems and Energy Efficient Technologies, Sumy State University, 2, Rymaskogo-Korsakova St., 40007 Sumy, Ukraine; ivanov@tmvi.sumdu.edu.ua

* Correspondence: svetlana.radchenko@tuke.sk



Citation: Loskutova, T.; Hatala, M.; Pogrebova, I.; Nikitina, N.; Bobina, M.; Radchenko, S.; Kharchenko, N.; Kotlyar, S.; Pavlenko, I.; Ivanov, V. Composition, Structure, and Properties of Ti, Al, Cr, N, C Multilayer Coatings on AISI W1-7 Alloyed Tool Steel. *Coatings* **2022**, *12*, 616. <https://doi.org/10.3390/coatings12050616>

Academic Editor:
Diego Martinez-Martinez

Received: 30 March 2022

Accepted: 28 April 2022

Published: 30 April 2022

Publisher’s Note: MDPI stays neutral with regard to jurisdictional claims in published maps and institutional affiliations.



Copyright: © 2022 by the authors. Licensee MDPI, Basel, Switzerland. This article is an open access article distributed under the terms and conditions of the Creative Commons Attribution (CC BY) license (<https://creativecommons.org/licenses/by/4.0/>).

Abstract: New methods of diffusion metallization of AISI W1-7 steel have been developed. The paper proposes a comparative analysis of the properties and characteristics of AISI W1-7 steel after three methods of chemical heat treatment: diffusion nitriding, nitrogen titration by physical deposition from the gas phase, and diffusion chromium plating with subsequent titanium alloys. The results are presented as a comprehensive analysis of coatings: metallographic, micro-X-ray spectral, X-ray phase, durometric, heat resistance, and wear resistance. It is established that multilayer protective coatings are formed as a result of treatments. It is shown that the coatings consist of carbide and nitride zones, intermetallic, and an Al₂O₃ layer outside the coating. The coatings have been found to contain barrier layers that prevent aluminum from penetrating the substrate. The maximum microhardness is typical for layers based on titanium carbide—30.3–35.5 GPa and titanium nitride—22.0–22.6 GPa, heat-resistant steels AISI W1-7 at a temperature of 900 °C in 4.2–8.5 times and wear resistance under sliding friction without lubrication up to 5.4 times compared to samples without treatment.

Keywords: titanium carbide; titanium nitride; chromium carbides; diffusion; barrier layer; heat resistance; wear resistance; coefficient of friction; industrial growth; process innovation

1. Introduction

Increasing the volume and efficiency of production during metal treatment is accompanied by the development of new and expanding the scope of existing types of tool complications during operation. This causes an increase in the tool’s temperature and the load in the contact area resulting in a reduction in product’s service life. Improving the stability of tools is now possible in the following way: improvement of design, development of new grades of alloys, and application of wear-resistant coatings.

It should be noted that from the economic standpoint of the technological capabilities of modern methods, it can be considered that the application of protective coatings is more promising than the development of new tool alloys.

Currently, there are some ways to obtain coatings on the working surfaces of steel and carbide tools [1–8]. After considering the peculiarities of the saturation processes, the following three methods can be distinguished: the method of physical deposition from the gas phase, the method of chemical deposition from the gas phase, and the method of chemical–thermal treatment, in which the formation of coatings is due to the diffusion processes of solid-phase, liquid, and gas-phase saturation.

Depending on the operational requirements, the gas-phase chemical deposition method is applied to the carbide plates with mechanical fastening multilayer coatings with the participation of TiN, TiC, and Al₂O₃ compounds [4,9,10]. The arrangement of the layers of compounds in the coating determines the advantage of a particular property. It is necessary to note that this technology's formation of nitride and carbide layers is due to the nitrogen–oxygen of the saturation medium. The obtained multilayer composition provides a complex of favorable properties: heat resistance, abrasive wear resistance, and resistance to indentation formation.

Using technologies of chemical–thermal treatment with a source of nitrogen–carbon to form, respectively, TiN and TiC layers will be the basis of tool steels. Nitrogen in steels or carbide may appear after nitriding. The results of studies on the formation of diffuser carbide and carbon–nitride coatings on tool steels and hard alloys are reported in [9,10]. Literature sources on the formation of TiN, TiC, and Al₂O₃ diffusive multilayer coatings on tool steels on hard alloys are unknown.

The coatings are also widely used in various technological fields. Particularly, the impact of diamond-like carbon coatings on the wear of the press joint components was studied in [11]. In addition, control of structural and phase transformations in Ti materials, WC–Co substrate, and Ti–Al coatings was studied in [12]. As a result, physicomechanical and wear properties were improved. Moreover, in [13], the influence of coatings on fretting wear in a clamped joint for ensuring the maintenance and reliability of structures has been investigated.

The quality of TiN coating on steels can be estimated from [14]. WC tungsten carbide and Co cobalt cutting tools have been the main components of hard alloy for decades. Concerns about cobalt toxicity have increased recently. This led to the search for new material for the binding phase [15]. At the same time, requirements for improving the quality of tools and working productivity in metalworking are increasing. In [14], it was shown that the deposition of TiN on iron causes strong corrosion of the substrate because of the formation of FeCl_x compounds in the gas phase. This is due to the exchange reactions between iron and TiCl₄ chloride. It is possible to assume the possibility of forming diffusion coatings without corrosion destruction of the steel surface during the reactions of titanium chloride disproportionation and elimination of reactions with the formation of iron chlorides [10].

Multilayer multicomponent coatings with aluminum are particularly interesting [16–18]. It can be assumed that in titanium aluminizing and chrome aluminizing, the coatings will combine the heat resistance of aluminum compounds with a hardness of carbides, titanium nitride, and chromium (TiN, TiC, Cr₇C₃, and Cr₂₃C₆) on the surface of carbon steel. The titanium alloys obtained by the powder method on the surface of carbon steels consist of a layer of TiC carbide outside the diffusion zone and a layer based on a solid Fe_α(Al) solution adjacent to the base. The latter's formation is due to the diffusion of aluminum through the layer of titanium carbide, dissolution of aluminum in austenite, and time of the maximum concentration and austenite flow Fe_γ → Fe_α transformation. A similar structure is formed on medium-carbon steel during chrome aluminizing. Layers of Cr₇C₃ and Cr₂₃C₆ carbides are formed on the surface; layers of FeAl Fe₃Al compounds are located closer to the base. The disadvantage of titanium alloy and chrome-aluminized coatings on the investigated steels is the poor location of the layers in the coating. Under

conditions of contact interaction, the composition is destroyed and does not realize the potential properties of hardness and heat resistance.

The functionality of the TiN, TiC, and Al₂O₃ compositions depends on the properties of the individual layers. It was shown in [19] that the TiN layer is consistently deposited in elections with good quality at a wide temperature range, even at low temperatures. There are difficulties in the precipitation of TiC compounds in forming carbon hydrides. During chemical deposition from the gas phase, the latter can consistently exist in a wide temperature range and thus inhibit the formation of TiC carbide. In addition, in the TiC layers, there are significant compressive stresses, which lead to the delamination of the coatings. The detachment of the coatings from the base is quite clear.

The purpose of the work is to determine the effects of the composition of the reaction medium and the composition of the surface of AISI W1-7 steel after prenitriding, predeposited by the method of physical deposition from the TiN gas-phase layer and a preapplied layer of chromium carbides Cr₇C₃ and Cr₂₃C₆ on phase, chemical composition, structure, thickness, and properties of the obtained coatings on AISI W1-7 steel.

2. Materials and Methods

2.1. Materials

AISI W1-7 tool steel was selected as the study object. The chemical composition of steel is given in Table 1. Ammonia was used as the starting reagents for nitriding; diffusion metallization used powders of saturating elements, namely, titanium powder size 100–300 µm, chromium powder with a size of 160–200 µm, and aluminum powder with a size of 150–300 µm. The chemical purity of the starting reagents of the powders was 95% and above. Carbon tetrachloride (CCl₄) or NH₄Cl was used as an activator. Inert Al₂O₃ backfill was used to prevent the sintering of powders during diffusion metallization by the contact powder method. The phase composition and the content of components in the saturating powder mixture are presented in Table 2.

Table 1. Chemical composition of AISI W1-7 steel.

No	The Content of Elements, % (wt.)								
1	C	Si	Mn	Cr	S	P	Cu	Ni	Fe
2	0.81	0.26	0.20	0.20	≤0.018	≤0.025	≤0.20	≤0.20	remainder

Table 2. Composition of the powder mixture, % (wt.).

No	Type of Treatment	The Phase Composition and Content of Components			
1	Titanium aluminizing	Ti (Cr) 40	Al 15	NH ₄ Cl 5	Al ₂ O ₃ 40
2	Chrominizing	55	-	5	40

2.2. Methods of Research

Titanium alloying was performed by powder method in a fusible container at a temperature of 1050 °C, and the process duration was 2–4 h. As starting reagents, mixtures of powders of the following composition (content in % wt.) 40-Ti, 15-Al, 5-NH₄Cl, and 40-Al₂O₃ were used. Titanium–chromium plating was performed as a gas method in a closed reaction space under reduced pressure conditions (13.3 Pa) in sealed containers using titanium, chromium, and carbon tetrachloride powders [9]. The last one was introduced into a saturated medium at a saturation temperature of 1050 °C. At nitriding, known nitriding technology in dissociated ammonia (25–35%) at 540 °C for 20 h was used.

Titanium nitride TiN of 5.0–5.5 µm thickness was obtained by physical deposition using the installation VU1B with titanium cathode with the following processing parameters: deposition time was 25 min; the substrate temperature at the beginning of the process

reached 560 °C, at the end 200 °C; the pressure in the reaction space was 2.5×10^{-2} Pa; resistance voltage 150 V; arc current 100 A.

The phase composition of the coatings was determined by X-ray spectral microanalysis (XRM) using a scanning electron microscope (REM) CamScan 4S (Obducat CamScan Ltd., Cambridge, UK), equipped with energy-dispersive EDX attachment-spectrometer Link Pentafet (Oxford Instruments, Abingdon, UK) and INCA-200 software (version 7.2). The operating accelerating voltage of REM for XRM is 20 kV. The cobalt spectrometer was calibrated before performing the XRM analysis every 2 h. The accuracy of quantitative XRM was $\pm 0.1\%$ wt. The content of all elements present in the coating and the base metal is determined by step scanning the sample under the electronic probe in the direction perpendicular to the side surface of the sample in the cross section of the section and XRM at points along the line along with the thickness of the coating with a step of 1–2 μm and areas located at different distances from the surface.

X-ray diffraction analysis was performed on the installation of DRON UM-1 in Cu $K\alpha$ -emitted ($\lambda = 0.154$ nm), processing the results on the program Powder Cell 2.2. Diffractograms from the surface of the samples were taken in the range of angles $2\theta = 25\text{--}85^\circ$, using the method of step scanning at a scanning step of 0.050 and exposure time at the point 5–7 s. The shooting was carried out on scales of 200–1000 pulses per second at a speed of movement of a chart tape of 1200 mm/h with a mark of angles through one degree. Layer-by-layer analysis of the samples was performed by mechanical grinding of the surface on a diamond wheel.

For studying the microstructure, sections of samples with the obtained coatings were made. The study of thin carbide, nitride, and intermetallic layers used the so-called “oblique sections”. PMT-3 devices in not less than 20 fields of view. The load on the indenter was 0.49 N. According to the obtained data, the average value of microhardness was determined.

Heat resistance was assessed by the change in mass of the samples after their oxidation at a temperature of 1000 °C for 85 h under conditions of natural aeration. Wear resistance under sliding friction conditions without lubrication according to the tab-shaft scheme was determined on an MT-68 friction machine (PJSC “Tochpribor”, Kharkiv, Ukraine) at a load of 5 N, 10 N, and 15 N, and a sliding speed of 10 m/s at room temperature. Hardened steel AISI 1066, hardness 51 HRC, was used as the counter body material.

The method of testing the scheme of the shaft tab allows analyzing the contact spot directly on the formed indentation wear. Wear during friction can be estimated by changing the mass of the sample or by changing the geometric parameters of the indentation.

The stability rate of the samples $K_M = \Delta m / (S \cdot \tau)$ was determined by the following parameters: Δm —change in mass of the test sample, kg; S —the surface area of the test sample, m^2 ; τ —duration of the test, h.

3. Results and Discussion

The results of studies of the phase and chemical compositions of the structure of the properties investigated in the work of coatings on AISI W1-7 steel are shown in Table 3, Figure 1.

Table 3. The phase composition and coating characteristics of AISI W1-7 steel (compounds zone).

Coating No	Type of Treatment; Temperature, °C; Time, h	Phase Composition	Lattice Period, nm	Coating Thickness, μm	Micro-Hardness, GPa
1	Titanizing; 1050; 3	FeTi	a: 0.2971	1.0–1.5	6.0
		Fe ₂ Ti	a: 0.4708 c: 0.7701	1.5–2.0	8.1
		TiC	a: 0.4328	16.0	37.8
2	Chrominizing, 1050; 4	FeCr	a: 0.8810 c: 0.5446	3.5	6.5–7.0
		Cr ₂₃ C ₆	a: 1.0658	6.0	16.5
		Cr ₇ C ₃	a: 0.4528 b: 0.7012 c: 1.2144	9.0	17.2
3	TiN, physical precipitation from gas phase	TiN	a: 0.4239	5.5–6.0	19.8
4	Nitriding in ammonia; 540; 16	Fe ₂ N	a: 0.4799	11.0	5.6
		Fe ₄ N	c: 0.4419 a: 0.3796	6.5	7.4
5	Titanium aluminizing *, 1050; Ti (40%), Al (15%), NH ₄ Cl (5%), Al ₂ O ₃ (40%)	Fe ₂ (Ti, Al) ₄ O	a: 1.1309	8.0	8.0
		TiC	a: 0.4330	5.0–5.5	34.5
		Fe α (Al)	a: 0.2800	35.0	2.0–2.9
6	Titanium aluminizing * of AISI W1-7 nitric steel	Fe ₂ (Ti, Al) ₄ O	a: 1.1295	10.0	11.1
		TiC	a: 0.4329	6.9	30.3
		TiN	a: 0.4240	5.0	22.0
7	Titanium aluminizing * of AISI W1-7 steel with a TiN layer	Fe ₂ (Ti, Al) ₄ O	a: 1.1293	10.0	11.1
		TiC	a: 0.4304	6.9	30.3
		TiN	a: 0.4240	5.0	22.0
8	Titanium aluminizing of AISI W1-7 chromium steel	AlCrTi	a: 0.5000	2.0	6.1–7.0
		Cr ₂ Ti	a: 0.6954	11.0	
		Ti ₃ Al	a: 0.5650 b: 0.5650 c: 0.4576	3.5	
		TiC	a: 0.4321	7.0	35.5
		Cr ₂₃ C ₆	a: 1.0711	5.5	16.0
		Cr ₇ C ₃	a: 0.6890 b: 1.2421 c: 0.4532	4.5	16.5

* Al₂O₃ was fixed on the surface.

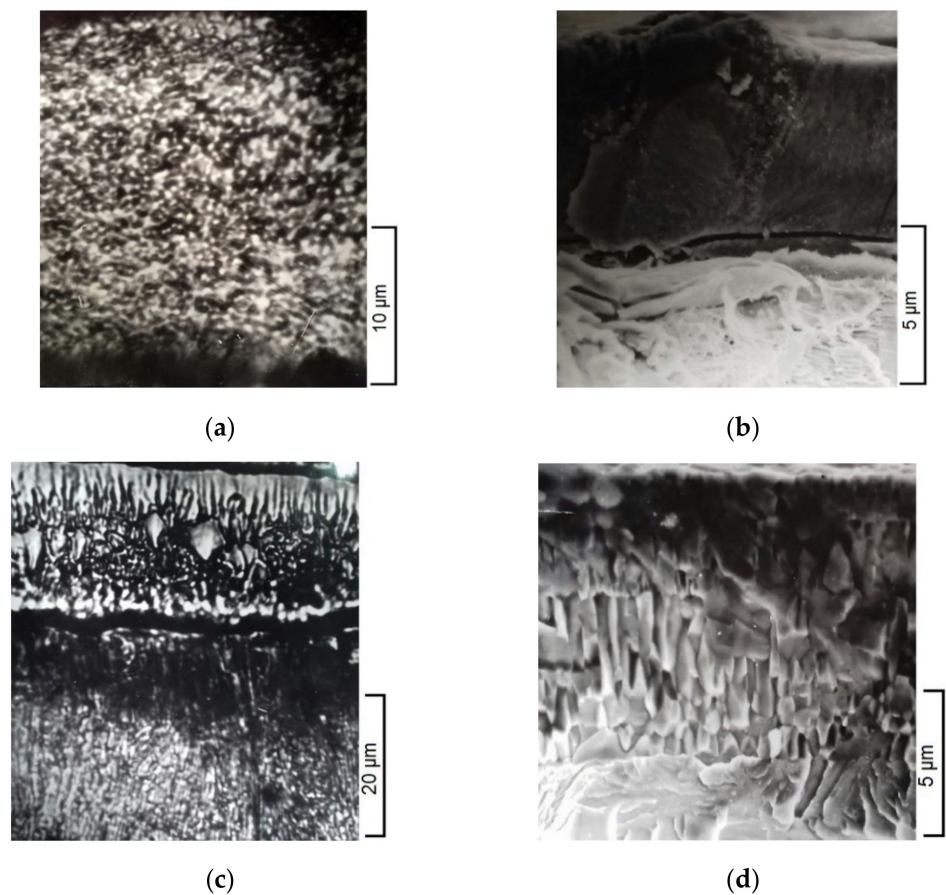


Figure 1. Microstructures of titanium (a,b) and chromium (c,d) coatings on AISI W1-7 steel: (a,c) light microscope; (a) $\times 1400$, (c) $\times 800$; (a) etching by Murakami solution; (b,d) raster microscope, by fractures.

The titanium coatings on AISI W1-7 steel consist, as already noted, of a layer of titanium carbide with a crystalline lattice period close to stoichiometric layers of intermetallic Fe_2Ti and FeTi , as well as a transition zone with high titanium content (Table 3). The TiC layer is formed along with the entire thickness of equilibrium grains of $0.5\text{--}0.7\ \mu\text{m}$. TiC fracture is transcrystalline. Pores are not detected in the structure (Figure 1).

As a result of X-ray diffraction analysis of AISI W1-7 steel after titanium aluminizing with TiN-(PVD) layer, it was found that a small amount of alumina Al_2O_3 is formed on the surface (Figure 2, Table 3). The main phase of the surface layer of the protective coating is FeTi_4O . X-ray diffraction analysis of AISI W1-7 steel at a distance of $10\ \mu\text{m}$ from the surface reveals the presence of two main phases: titanium carbide TiC and titanium nitride TiN.

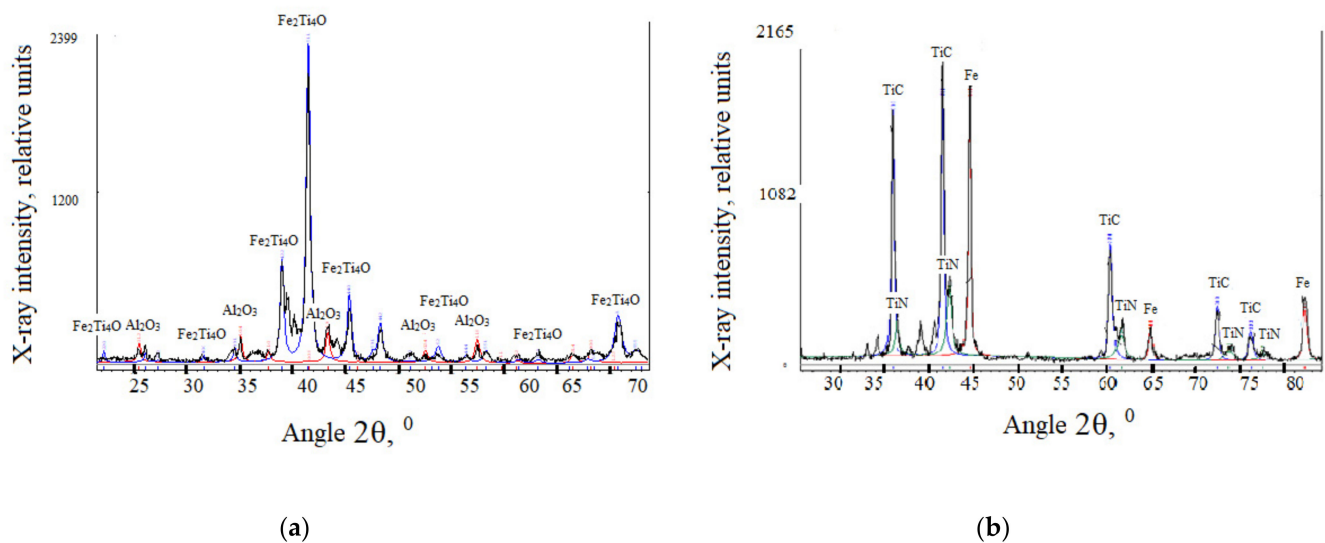


Figure 2. Diffractograms for AISI W1-7 steel with TiN-(PVD) layer after titanium aluminizing: (a) surface; (b) at a depth of 10 μm of the cut layer. Radiation Cu $K\alpha_1$, $\lambda = 0.154 \text{ nm}$.

The outer layer of intermetallic (σ -phase) and the transition zone is characteristic of chromium coatings. In this case, the layers of Cr_7C_3 and Cr_{23}C_6 carbides in the light microscope and raster microscope are revealed with a columnar structure (Figure 1c,d).

Part of the samples, before titanium alloying, was applied by physically precipitating, from the gas phase, the titanium nitride TiN thickness of 4.5–5.0 μm . The TiN compound layer is yellow in a light microscope, corresponding to a stoichiometric nitride composition. The latter is confirmed by X-ray analysis, according to which the period of the FCC lattice of the compound TiN is 0.4245 nm (Table 3).

Nitriding occurred in ammonia at 25–35% dissociation at 540 $^\circ\text{C}$ for 20 h. A diffusion layer is formed during the process of treatment on the surface of AISI W1-7 steel, which consists of a zone of compounds: these are the layers of Fe_4N , Fe_{2-3}N , phases, as well as the internal nitriding zone (Table 3). The last in the pearlitic structure of AISI W1-7 steel is practically undetectable.

The titanium alloys are formed by the simultaneous saturation of titanium and aluminum in the powder mixture consisting of a solid solution of $\text{Fe}_\alpha(\text{Al})$ at the boundary with the base. The layers of TiC and $\text{Fe}_2(\text{Al}, \text{Ti})_4\text{O}$ are formed outside. The $\text{Fe}_\alpha(\text{Al})$ layer was formed during the diffusion of aluminum into austenite due to the polymorphic $\text{Fe}_\gamma \rightarrow \text{Fe}_\alpha$ transformation. At a temperature of 1050 $^\circ\text{C}$, the conversion of austenite into ferrite occurs at an aluminum content of 0.5–0.8% mass. Because of the low solubility of carbon in ferrite, carbon is displaced from the surface (Table 3). TiC layers are formed by diffusion of the substrate carbon to the surface by adsorbed titanium. Over time, the growth rate of the TiC layer decreases. This effect allows forming compounds with iron on the outside. In the same way, $\text{Fe}_2\text{Ti}_4\text{O}$ layers are formed in steels by diffusion from the Fe base.

After etching with a 3% alcohol solution of nitric acid, the $\text{Fe}_\alpha(\text{Al})$ layer appears as a light zone with characteristic column crystals (Figure 3). It should be noted that titanium is practically absent in the layer of $\text{Fe}_\alpha(\text{Al})$ both at some distance from the TiC layer and directly beyond the boundary of TiC– $\text{Fe}_\alpha(\text{Al})$ layers.

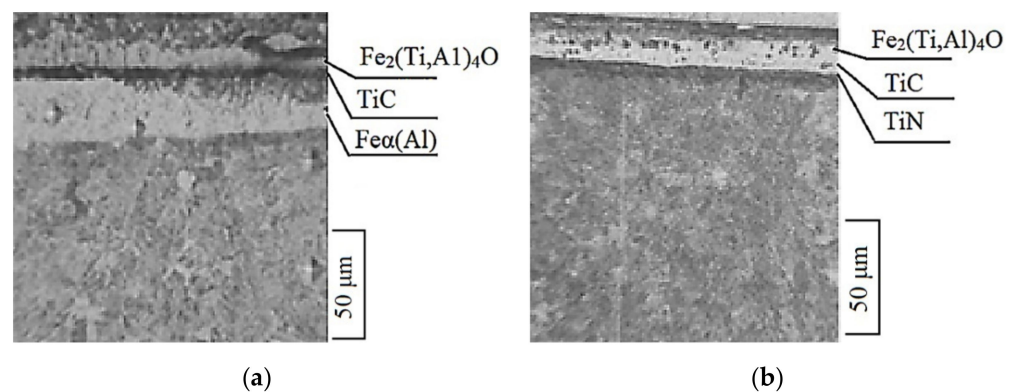


Figure 3. Microstructures of titanium aluminized coatings on AISI W1-7 steel; (a,b) light microscope; $\times 300$; (b) a layer of TiN applied to AISI W1-7 steel before the titanium aluminizing; titanium aluminizing ($1050\text{ }^\circ\text{C}$, 4 h).

The absence of titanium is caused by its interaction on the surface with the carbon base and a layer based on TiC carbide. It is essential to mention that aluminum does not form carbides in the diffusion zone under acceptable conditions but diffuses through the TiC layer into the base where the $Fe_\alpha(Al)$ layer is formed. The aluminum concentration on the surface of AISI W1-7 titanium alloy steel and in $Fe_\alpha(Al)$ solid solution is 19.8 and 7.5–8.5% wt., respectively.

A common feature of multilayer coatings obtained by nitriding methods, physical precipitation from the gas phase, and diffusion chromium plating with titanium alloying is the obtained coating layer of TiC compounds (coating 6–8, Table 3). TiC carbide in these coatings is formed from the carbon diffusion from the base and the interaction on the surface with titanium. The thickness of the TiC layers in coatings 6–8 (Table 3) is less than the thickness of the TiC layer in coating 1 (Table 3) because of the presence in the coatings 6–8 (Table 3) of the intermediate zone with barrier functions; these are layers TiC in coatings 6 and 7 (Table 3), and layers Cr_7C_3 and $Cr_{23}C_6$ in coating 8 (Table 3). TiN layer in coating 6 (Table 3) begins to form in the initial stages of titanium alloying, and its barrier properties increase with thickness, which causes a slightly larger thickness of the TiC layer compared with the thickness of the TiC layer in coating 7 (Table 3).

The difference between the phase composition of coatings No 6–8 (Table 3) from titanium alloy No 5 (Table 3) is the absence of a layer of Fe (Al). This fact is due to the presence of barrier TiN layers in coatings No 6 and 7 (Table 3) and layers Cr_7C_3 and $Cr_{23}C_6$ in coating No 8 (Table 3), which completely stop the penetration of aluminum into the steel substrate. The $Fe\alpha(Al)$ layer was not detected in the coating data after titanium alloying. In the coatings No 6 and 7 (Table 3), carbon and iron diffuse through the TiN and TiC layers from the base to the surface.

The analysis of the obtained data showed the effect of titanium aluminizing on the phase composition of the nitrided and chromium layers, which becomes almost unchanged after titanium alloying of the TiN layer. The layers of Fe_4N , Fe_3N , and Fe_3O_4 compounds disappear on nitrous steel, and the composition of the internal nitriding zone changes. In the chromium coating of Cr_7C_3 , $Cr_{23}C_6$, and σ -phase carbides, the following changes occur: the total thickness of the carbide layer decreases from 15.0 to 10.0 μm mainly because of the thickness of the Cr_7C_3 layer; the σ -phase layer disappears.

These research results suggest that the carbon source for TiC formation is chromium carbide carbon, not the base carbon. Thus, the formation of the TiC layer occurs during the dissociation of chromium carbides. Thus, released carbon diffuses to the surface and participates in the formation of the TiC layer. Chromium and iron, together with the saturating elements of titanium and aluminum, form the compounds of the outer layers $AlCrTi$, Cr_2Ti , and Ti_3Al .

The crystalline lattice periods of TiC titanium carbide and TiN titanium nitride correspond to compounds close in composition to stoichiometric [20,21]. It is known [21] that the period of TiN crystalline lattice increases with increasing nitrogen content in the homogeneity region, which changes at 1400 °C from TiN 0.6 to TiN 1.0. It was found that the lattice period of the TiN phase of the penetration obtained by physical deposition on AISI W1-7 steel practically did not change after the subsequent titanium alloying and was higher than the lattice period of TiN formed after the titanium alloying of nitrous steel. The latter may indicate a lack of nitrogen source power (nitrous steel). In this case, the lattice period of the TiC layer on nitrous steel (coating No 6, Table 3) was a more considerable period of the lattice TiC on steel with a layer of TiN (coating No 7, Table 3). The established dependence can be explained by the inhibition of carbon flux from the base to the surface by a layer of TiN and the absence of such a layer on the samples with coating No 6 (Table 3).

Analysis of the results of studies of the phase composition showed that the layers of TiC and TiN in coatings 1, 5–8 (Table 3) are formed by the extraction of titanium carbon and nitrogen to the surface with the formation of phases of penetration. TiN coatings acting as an aluminum barrier prevent the formation of a $Fe\alpha(Al)$ layer. In addition, titanium aluminizing may lead to TiC, TiN by iron, and chromium layers, which diffuse to the surface through these layers.

So, the concentration of aluminum and iron in the layer of TiC in conventional titanium alloy (coating No 5, Table 3) is aluminum at the level of 0.2% and has 2.4–4.6% wt. Simultaneously, the aluminum content on the outside of the coatings No 5–8 (Table 3) is 18.5–19.8% of the mass, iron 20.0–38.0% wt. Titanium alloying nitrous steel with a layer of TiN increases the TiC layer of aluminum content to 0.5–0.6% wt. and reduces the iron content to 1.1% wt. The aluminum content in the TiN layer reaches 1.3–1.4% wt., and iron—2.3–2.4% wt.

Figures 4 and 5 show the results of studies of the distribution of saturating elements and substrate elements by the thickness of titanium alloy coatings on AISI W1-7 nitrous steel and a distribution map. As already noted, the main difference between coatings No 5 and coatings 6–8 (Table 3) is the lack of coatings 6–8 (Table 3) $Fe\alpha(Al)$ layer. The established feature of the structure of coatings 6–8 is the presence of barrier layers, which inhibit the penetration of aluminum into the substrate and prevent the formation of the $Fe\alpha(Al)$ layer.

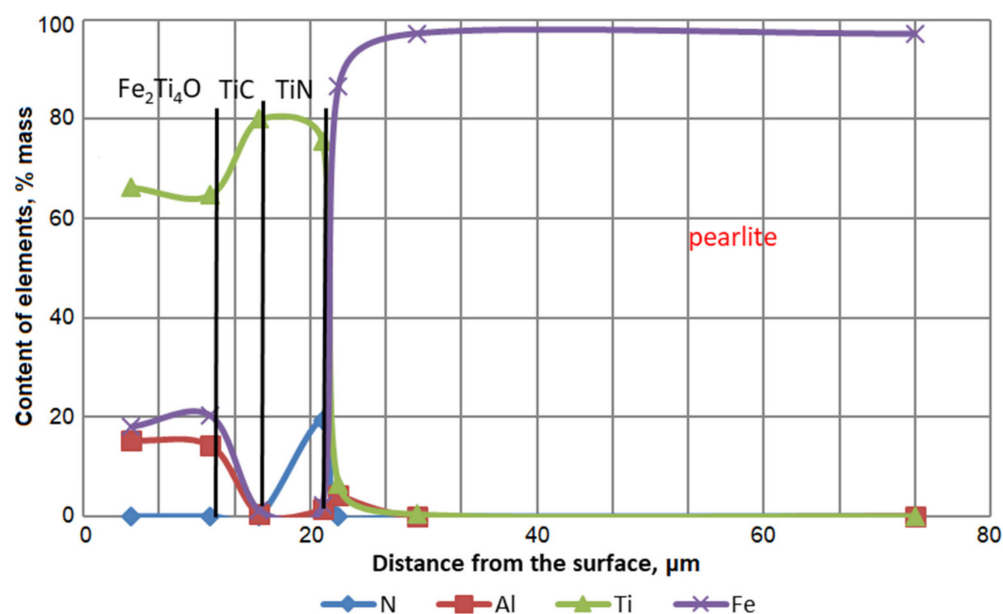


Figure 4. Distribution of elements in titanium aluminized coatings on AISI W1-7 nitrous steel; nitriding (540 °C, 36 h); titanium aluminizing (1050 °C, 4 h).

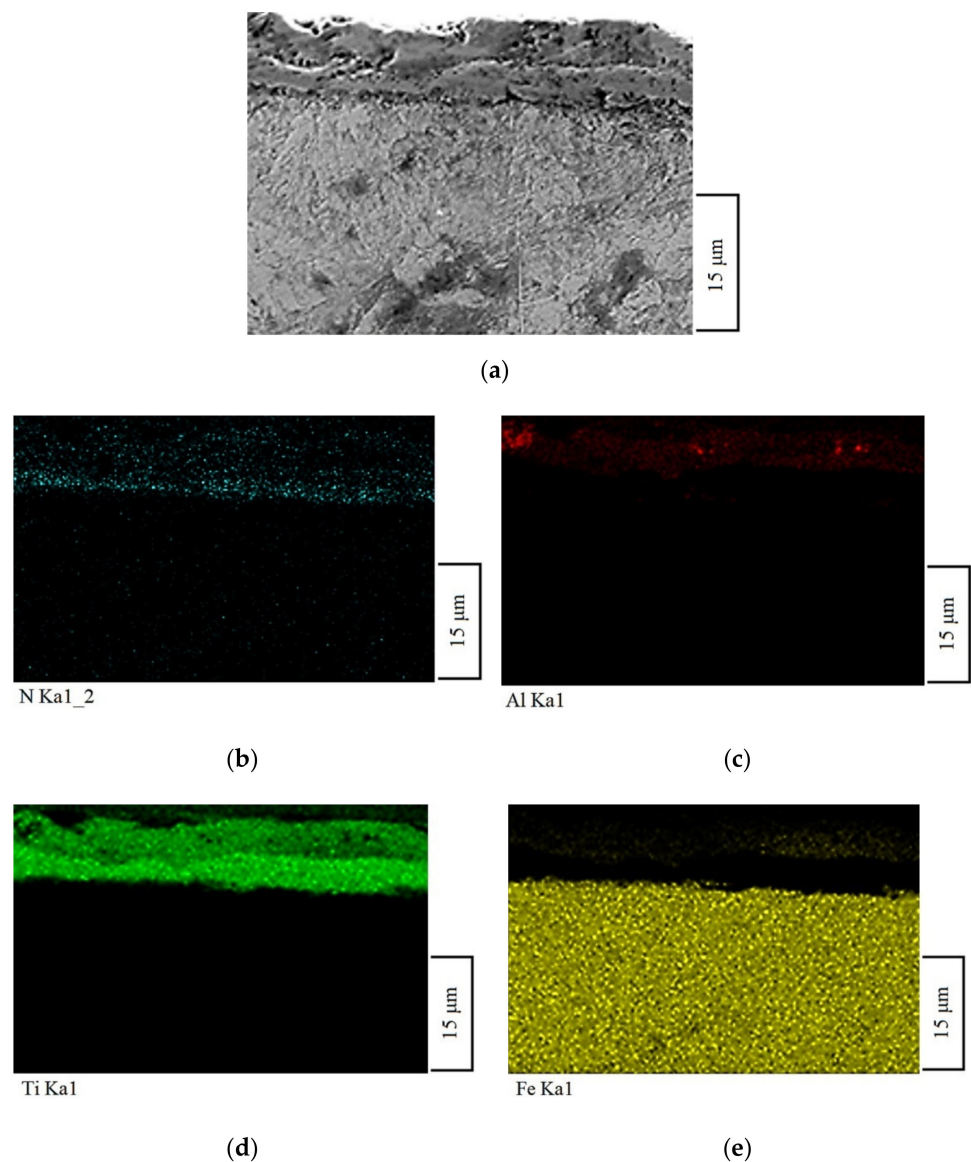


Figure 5. Microstructure in reflected electrons (a) and distribution map of elements along the plane of grinding on AISI W1-7 steel (characteristic X-ray radiation in secondary electrons) for N (b), Al (c), Ti (d), Fe (e) after nitrous titanium aluminizing: nitriding (540 °C, 36 h), titanium aluminizing (1050 °C, 4 h).

In the $\text{Fe}_2(\text{Ti}, \text{Al})_4\text{O}$ layer, a significant amount of nitrogen was revealed. The nitrogen source can be in samples No 6 (Table 3), nitrogen residues in steel after titanium, titanium nitride, and in samples No 7 (Table 3)—titanium nitride. Titanium nitride nitrogen diffuses to the surface and dissolves in a layer of $\text{Fe}_2(\text{Ti}, \text{Al})_4\text{O}$. The solubility of titanium nitride in $\text{Fe}_2\text{Ti}_4\text{O}$ was shown in [22], in which the $(\text{Ti}, \text{Zr})\text{N}$ compound was used as a barrier layer. Probably in equilibrium with the TiC layer, there must be a compound with certain nitrogen content. Thus, the TiN layer is dissociated during the chemical–thermal treatment, followed by the diffusion of nitrogen and titanium into the $\text{Fe}_2\text{Ti}_4\text{O}$ layer.

Figure 6 shows the results of the studies of the distribution of elements by the thickness of coating No. 5 (Table 3) and coatings obtained by diffusion titanium aluminizing of chromium steel. According to the results obtained in coating No 8 (Table 3), titanium alloying is the dissociation of chromium carbides, which is confirmed by reducing the thickness of their layers. The carbon released from chromium carbides interacts with

titanium to form TiC carbide, and chromium interacts with the metal. The thickness of the TiC layer in coating No 8 (Table 3) is 7.0 μm .

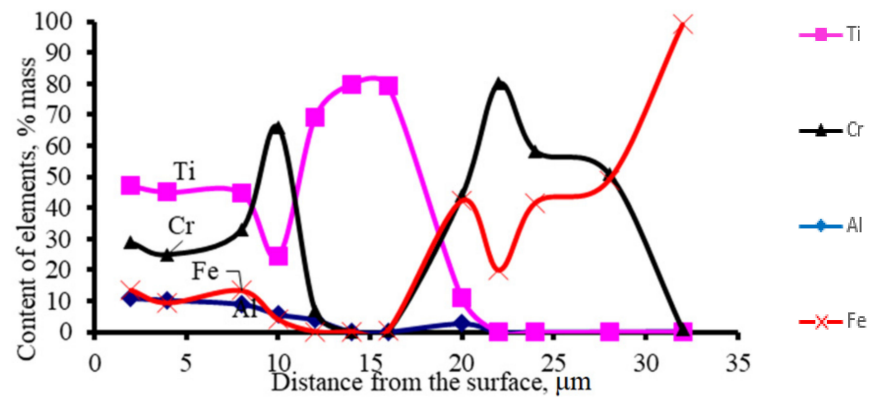


Figure 6. Elements distribution by the thickness of the coating of AISI W1-7 steel with a layer of σ -phase; Cr_7C_3 and Cr_{23}C_6 after titanium aluminizing: chromizing (1050 $^\circ\text{C}$, 4 h); titanium aluminizing (1050 $^\circ\text{C}$, 4 h).

Metallographic analysis of the obtained coatings showed a significant difference between complex coatings with TiN nitride layers and chromium carbides (coatings 6–8, Table 3). First of all, this concerns the absence and complex coatings of the $\text{Fe}\alpha(\text{Al})$ layer. Directly to the base in coatings 0 and 7 (Table 3) is the adjacent layer of TiN or a layer of chromium carbides in coating No 8 (Table 3). Outside there is a layer of titanium carbide TiC and a layer of $\text{Fe}_2(\text{Ti}, \text{Al})_4\text{O}$ in coatings No 6 and 7 (Table 3), or a layer of TiC and layers of intermetallics in coating No 8 (Table 3).

It should be noted that the TiN nitride layer is well identified in the structure during analysis and light microscope because of its yellow-gold color.

The microhardness of individual component coatings varies over a wide range: from the microhardness of TiC carbide layers—30.3–37.8 GPa, TiN nitride—19.8–22.0 GPa, of Cr_7C_3 carbides and Cr_{23}C_6 —16.5–17.2 GPa, to microhardness of intermetallics, oxides—6.1–14.0 GPa. The microhardness of the outer layers in the TiN coatings (No 6, 7, Table 3) was higher than the microhardness of the similar layers in coatings No 5. This fact is due, as already mentioned, to the alloying of these zones in coatings No 6 and 7 (Table 3) with nitrogen.

Analysis of test results of coatings investigated in the work showed that the heat resistance of AISI W1-7 steel with coatings increased 4.2–8.5 times (Figure 7). The maximum heat resistance was shown by coating No 8 (Table 3) obtained by titanium alloying of chromium steel. Analysis of the literature sources [23,24] shows that at elevated temperatures under continuous oxidation of Ti–Al–Cr alloys on the surface, an oxide film $(\text{Al}, \text{Cr})_2\text{O}_3$ is formed at high oxidation resistance. The properties of coatings with the participation of titanium on aluminum at high temperatures, under conditions of friction of the sliding, depend on the presence on the outside of the layer of compound Al_2O_3 [23,24]. Increasing the heat resistance of coatings with titanium and aluminum is important. The heat resistance of titanium and aluminum alloys depends on the composition and increases with increasing aluminum content up to 60–70% wt. In this case, the binary Ti–Al alloy with significant aluminum content becomes brittle, limiting its practical use. This solution is made possible by using chromium as an alloying element. Ti–Al–Cr alloys consisting of the Laves $\text{Ti}(\text{Al}, \text{Cr})_2$ and θ -phase ($\text{Ti}_{0.25}\text{Al}_{10.67}\text{Cr}_{0.08}$) are characterized by high heat resistance and mechanical properties [23,24]. First of all, it is an alloy containing 25–35% of the Laves phase and 70–75% having the θ -phase.

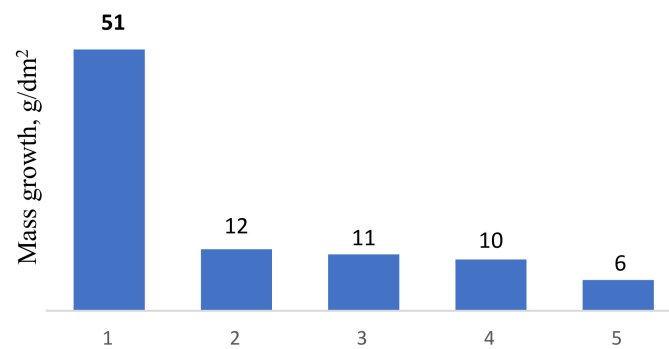


Figure 7. Heat resistance of AISI W1-7 steel (1000 °C; 85 h): 1—AISI W1-7 steel; 2—Cr₇C₃, Cr₂₃C₆ coatings; 3—titanium nitriding; 4—TiN layer with titanium aluminizing; 5—the layer of chromium carbides with titanium aluminizing.

The oxidation of compounds involving titanium and aluminum occurs by forming an oxidation zone, the phase composition of which depends on the content of aluminum in the coating and temperature [25–27]. In Ti_xAl_xN films [26], the aluminum content was changed from 25.0 to 67.0% wt. The heat resistance, in this case, increased. The oxidation of the TiAlN film aggregates at 700 °C and below is accompanied by the heterogeneous zone of the oxides Al₂O₃ and TiO₂. At temperatures above 800 °C, the heat resistance increases, and a two-layer oxide structure is formed from the Al₂O₃ compounds—the outer layer and the inner layer TiO₂. Al₂O₃ layer performs the main protective functions.

The aluminum stock determines the heat resistance of the coating material. The higher the aluminum content, the longer the coating service life. When tested, the aluminum part of the coating forms an Al₂O₃ oxide film. The part diffuses into the substrate. In addition, it is possible to diffuse the base elements in the coating, which also reduces the concentration of aluminum. The results show that the TiN barrier layer almost completely blocks aluminum diffusion to the base. It was shown in [27] that the amount of aluminum transferred from the coating to the substrate is the same as the coating in Al₂O₃ oxide.

Analysis of the results of studies of AISI W1-7 steel wear resistance with multicomponent coatings in the conditions of sliding friction without lubrication for the accepted sliding speed (10 m/s) and loadings (5.0, 10.0, and 15.0 N) showed the feasibility of using developed coatings for tool protection (Figure 8). Titanium alloy coatings showed the highest wear resistance with preapplied layers of chromium carbides and titanium nitride.

Sliding friction on the contact surfaces of solids at full pressure occurs in small areas of the so-called contact spots [28,29]. The total area of contact spots corresponds to the actual contact area, which is a small fraction of the nominal one. In the friction process, the shape and position of the contact spots are constantly changing. Studies have established [29] that the average diameter of contact spots is 6.0–30.0 μm at a distance between them of 80.0–120.0 μm.

Notably, individual properties and characteristics of coatings have been positively affected. The actual working conditions of the cutting tool are complex, while some physical and chemical processes occur, which lead to the destruction of the product. The paper discusses some processes related to the impact on the wear resistance of barrier coatings based on TiN titanium nitride.

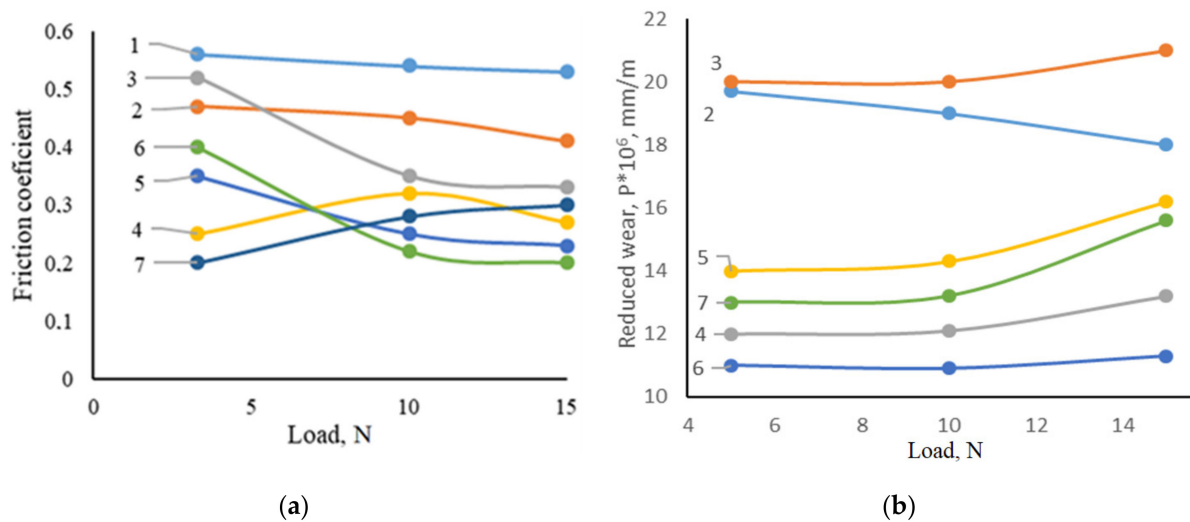


Figure 8. Dependence of friction coefficient (a) and reduced wear (b) on slip load AISI W1-7 of steel (1), AISI W1-7 chromium steel (2), AISI W1-7 nitrous steel (3), titanium aluminized with Cr_7C_3 , Cr_{23}C_6 layer (4), titanium aluminized (5), titanium aluminizing after nitriding (6), titanium aluminizing with TiN (7). The sliding speed is 10 m/s; the reduced wear of AISI W1-7 steel (HRC 62) at loads of 3.0, 10.0, and 15.0 N are equal to 43.0, 53.0, and 59.0, respectively; the sliding speed is 10 m/s.

The temperature in the area of contact interaction during cutting can reach significant values, accompanied by the interaction of the coating elements and the substrate with the environment. Formed oxide films, which are well bonded to the substrate and have anti-friction properties, increase the wear resistance of the tools. The formation of oxides of the desired composition is possible only on an alloy of a particular composition. It is known that the wear resistance of multicomponent coatings is positively influenced by the layers of Al_2O_3 aluminum oxide and TiO_2 titanium oxide. A layer of Al_2O_3 alumina was fixed on the surface of the coating after chemical–thermal treatment partially formed during the friction process. A layer of TiO_2 oxide is formed in testing at increased temperatures. It can be assumed that the presence of a barrier layer based on TiN titanium nitride stabilizes the chemical composition by inhibiting the diffusion drainage at the base of the coating elements, primarily aluminum. In addition, the barrier layers inhibit the diffusion of the coating elements into the treated alloy and the processed alloy (counter) elements into the coating.

The properties of the coatings and their structure are formed by the friction layers of aluminum and titanium oxides, causing a decrease in the friction coefficients of AISI W1-7 steel with coatings in contact with the rider and thus contributing to the increase in wear resistance. The coefficient of friction was determined in the conditions of the formed indentation wear, which corresponds to the actual operating conditions of the cutting tools. An analysis of the literature [30,31] showed the effect of coatings on the coefficient of friction during tests under sliding friction conditions without lubrication according to the scheme of the pin-disk. It is established that the coating of TiN titanium nitride in friction with steel contributes to reducing the coefficient of friction compared with the coefficient of friction of steel pair by 2.1 times. In the same work [31], TiN coatings reduce the friction coefficient to a small extent, and even the chromium carbide coatings increase.

Under the considered friction conditions, an indentation with a depth more significant than the thickness of the coating is formed in the contact zone. Thus, the indentation edges will consist of layers of TiN, TiC, intermetallics, and oxides Al_2O_3 and TiO_2 . The central zone of the indentation corresponds to the base material with possible inclusions of the destroyed coating—TiN and TiC particles, which corresponds to the Sharpey structure. The proposed complex coatings, by their structure and properties, can enhance the functional properties of AISI W1-7 tool steel.

4. Conclusions

The results of studies of new generation coatings with barrier layers based on titanium nitride TiN and chromium carbides Cr_7C_3 and Cr_{23}C_6 on AISI W1-7 tool steel are presented in this article:

1. The possibility of titanium aluminizing of AISI W1-7 steel with precoated methods of chemical–thermal treatment is shown, including diffusion chromium with carbide layers of Cr_7C_3 and Cr_{23}C_6 , and nitriding as well as physical gas deposition methods of TiN layer. The obtained coatings are chromium carbides Cr_7C_3 , Cr_{23}C_6 , TiC titanium carbide, TiN titanium nitride, and intermetallics with Ti, Al, Cr, and Fe. Layers of chromium carbides and TiN titanium nitride act as barriers that prevent the penetration of aluminum into the steel base and inhibit the formation of compounds under the $\text{Fe}\alpha(\text{Al})$ layer;
2. The maximum microhardness was found for TiC layers, 30.3–35.5 GPa, and TiN layers, 22.0–22.6 GPa. The maximum microhardness of the $\text{Fe}_2(\text{Ti, Al})_4\text{O}$ layer was found for the nitrogen titanium aluminized coating, 14.0 GPa, because of the presence of nitrogen;
3. The obtained coatings increase the heat resistance of AISI W1-7 steel at a temperature of 900 °C by 4.2–8.5 times and wear resistance under sliding friction conditions without lubrication up to 5.4 times. Maximum heat resistance showed coatings obtained by titanium alloying of chrome-plated steel. The advantage of coatings containing chromium is due to the formation during oxidation of high-quality protective film $(\text{Al, Cr})_2\text{O}_3$. Under the same oxidation conditions, a less dense, loose film of TiO_2 and Al_2O_3 oxides with unsatisfactory protective properties is formed on the surface of titanium alloy coatings. The high wear resistance of the coatings studied in this work is due to their structure and high microhardness of the individual components: the presence of layers TiC, TiN, Cr_7C_3 , Cr_{23}C_6 , intermetallics, TiO_2 , Cr_2O_3 , and Al_2O_3 . The properties of coatings and their structure, formed by friction layers of aluminum and titanium oxides, cause a decrease in the coefficients of friction of AISI W1-7 steel with coatings in contact with the counterweight and thus contribute to increased wear resistance.

Author Contributions: Conceptualization, T.L. and I.P. (Inna Pogrebova); methodology, M.B. and S.R.; software, M.H. and N.K.; validation, S.K. and I.P. (Ivan Pavlenko); formal analysis, T.L. and V.I.; investigation, I.P. (Inna Pogrebova), M.B. and S.R.; resources, M.H. and N.K.; data curation, S.K.; writing—original draft preparation, N.N., S.R., I.P. (Ivan Pavlenko) and V.I.; writing—review and editing, N.N.; visualization, V.I.; supervision, M.H. and I.P. (Ivan Pavlenko); project administration, T.L. and M.H.; funding acquisition, M.H. All authors have read and agreed to the published version of the manuscript.

Funding: This work was funded by the Slovak Research and Development Agency under contract No APVV-20-0514 and the projects VEGA 1/0391/22, KEGA 014TUKE-4/2020 were granted by the Ministry of Education, Science, Research and Sport of the Slovak Republic.

Institutional Review Board Statement: Not applicable.

Informed Consent Statement: Not applicable.

Data Availability Statement: The data presented in this study are available on request from the corresponding author.

Acknowledgments: The results have been obtained within the project “Fulfillment of tasks of the perspective plan of development of a scientific direction “Technical sciences” Sumy State University” supported by the Ministry of Education and Science of Ukraine (State reg. No. 0121U112684). The research was partially supported by the Research and Educational Center for Industrial Engineering (Sumy State University) and International Association for Technological Development and Innovations.

Conflicts of Interest: The authors declare no conflict of interest.

References

1. Bitay, E.; Tóth, L.; Kovács, T.A.; Nyikes, Z.; Gergely, A.L. Experimental Study on the Influence of TiN/AlTiN PVD Layer on the Surface Characteristics of Hot Work Tool Steel. *Appl. Sci.* **2021**, *11*, 9309. [[CrossRef](#)]
2. Inoue, S.; Uchida, H.; Hioki, A.; Koterazawa, K.; Howson, R.P. Structure and composition of (Ti, Al)N films prepared by r.f. planar magnetron sputtering using a composite target. *Thin Solid Films* **1995**, *271*, 15–18. [[CrossRef](#)]
3. Jehn, H.A. Multicomponent and multiphase hard coatings for tribological applications. *Surf. Coat. Technol.* **2000**, *131*, 433–440. [[CrossRef](#)]
4. Kohlscheen, J.; Bareiss, C. Effect of hexagonal phase content on wear behaviour of AlTiN arc PVD coatings. *Coatings* **2018**, *8*, 72. [[CrossRef](#)]
5. Su, J.; Boichot, R.; Blanquet, E.; Mercier, F.; Pons, M. Chemical vapor deposition of titanium nitride thin films: Kinetics and experiments. *CrystEngComm* **2019**, *21*, 3974–3981. [[CrossRef](#)]
6. Arai, T.; Moriyama, S. Growth behavior of chromium carbide and niobium carbide layers on steel substrate, obtained by salt bath immersion coating process. *Thin Solid Films* **1995**, *259*, 174–180. [[CrossRef](#)]
7. Fan, X.S.; Yang, Z.G.; Zhang, C.; Zhang, Y.D.; Che, H.Q. Evaluation of vanadium carbide coatings on AISI H13 obtained by thermo-reactive deposition/diffusion technique. *Surf. Coat. Technol.* **2010**, *20*, 641–646. [[CrossRef](#)]
8. Chabak, Y.G.; Fedun, V.I.; Pastukhova, T.V.; Zurnadzhy, V.I.; Berezhnyy, S.P.; Efremenko, V.G. Modification of steel surface by pulsed plasma heating. *Probl. At. Sci. Technol.* **2017**, *110*, 97–102.
9. Oskolkova, T.N.; Glezer, A.M. Surface hardening of hard tungsten-carbide alloys: A review. *Steel Transl.* **2017**, *47*, 788–796. [[CrossRef](#)]
10. Kostyk, K.; Kuric, I.; Saga, M.; Kostyk, V.; Ivanov, V.; Kovalov, V.; Pavlenko, I. Impact of magnetic-pulse and chemical-thermal treatment on alloyed steels' surface layer. *Appl. Sci.* **2022**, *12*, 469. [[CrossRef](#)]
11. Kowalski, S. Influence of diamond-like carbon coatings on the wear of the press joint components. *Wear* **2021**, *486–487*, 204076. [[CrossRef](#)]
12. Kameneva, A.; Antonova, N.; Pesin, M.; Makarov, V.; Nikitin, S.; Bublik, N. Structural and phase transformations control in Ti and Al cathode materials, WC-Co substrate, and Ti_{1-x}Al_xN coating to improve their physico-mechanical and wear properties. *Int. J. Refract. Met. Hard Mater.* **2022**, *102*, 105726. [[CrossRef](#)]
13. Kowalski, S. The influence of selected PVD coatings on fretting wear in a clamped joint based on the example of a rail vehicle wheel set. *Ekspluat. Niezawodn.* **2018**, *20*, 1–8. [[CrossRef](#)]
14. Von Fieandt, L.; Larsson, T.; Lindahl, E.; Bäcke, O.; Boman, M. Chemical vapor deposition of TiN on transition metal substrates. *Surf. Coat. Technol.* **2018**, *334*, 373–383. [[CrossRef](#)]
15. Richter, V.; Potthoff, A.; Pompe, W.; Gelinsky, M.; Ikonomidou, H.; Bastian, S.; Schirmer, K.; Scholz, S.; Hofinger, J. Evaluation of health risks of nano- and microparticles. *Powder Met.* **2008**, *51*, 8–9. [[CrossRef](#)]
16. Chen, J.-K.; Chen, S.-F.; Huang, C.-S. Formation of Al and Cr dual coatings by pack cementation on SNCM439 steel. *ISIJ Int.* **2012**, *52*, 127–133. [[CrossRef](#)]
17. Geib, F.D.; Rapp, R.A. Simultaneous chromizing–Aluminizing coating of low-alloy steels by a halide-activated, pack-cementation process. *Oxid. Met.* **1993**, *40*, 213–228. [[CrossRef](#)]
18. Mei, S.Q.; Guryev, A.M.; Ivanov, S.G.; Lygdenov, B.D.; Tsydygov, B.S.; He, X.Z.; Liang, Q.Y. Research on the chance of increasing the wear resistance of high-speed steel using chemical thermal treatment methods. *IOP Conf. Ser. Mater. Sci. Eng.* **2019**, *479*, 012055. [[CrossRef](#)]
19. Petkov, N.; Bakalova, T.; Bahchedzhiev, H.; Louda, P.; Kejzlar, P.; Capkova, P.; Kormunda, M.; Rysanek, P. Cathodic arc deposition of TiCN coatings-influence of the C₂H₂/N₂ ratio on the structure and coating properties. *J. Nano Res.* **2018**, *51*, 78–91. [[CrossRef](#)]
20. Trotsan, A.I.; Kaverinskii, V.V.; Brodetskii, I.L. Use of fine powders of refractory carbides and nitrides for inoculation of iron-carbon alloys. *Powder Metall. Met. Ceram.* **2014**, *52*, 600–605. [[CrossRef](#)]
21. Fan, Y.; Li, L.; Zhang, Y.; Zhang, X.; Geng, D.; Hu, W. Recent advances in growth of transition metal carbides and nitrides (MXenes) crystals. *Adv. Funct. Mater.* **2022**, *2022*, 2111357. [[CrossRef](#)]
22. Zhu, L.; Feng, C.; Zhu, S.; Wang, F.; Yuan, J.; Wang, P. Comparison of CrN, AlN and TiN diffusion barriers on the interdiffusion and oxidation behaviors of Ni+CrAlYSiN nanocomposite coatings. *Crystals* **2021**, *11*, 1333. [[CrossRef](#)]
23. Fox-Rabinovich, G.S.; Wilkinson, D.S.; Veldhuis, S.C.; Dosbaeva, G.K.; Weatherly, G.C. Oxidation resistant Ti-Al-Cr alloy for protective coating applications. *Intermetallics* **2006**, *14*, 189–197. [[CrossRef](#)]
24. Zhou, C.; Yang, Y.; Gong, S.; Xu, H. Effect of Ti–Al–Cr coatings on the high temperature oxidation behavior of TiAl alloys. *Mater. Sci. Eng. A* **2001**, *307*, 182–187. [[CrossRef](#)]
25. Grachev, V.A.; Rozen, A.E.; Perelygin, Y.P.; Kireev, S.Y.; Los, I.S. Multilayer corrosion-resistant material based on iron–carbon alloys. *Heliyon* **2020**, *6*, e04039. [[CrossRef](#)]
26. Joshi, A.; Hu, H.S. Oxidation behavior of titanium-aluminium nitrides. *Surf. Coat. Technol.* **1995**, *76–77*, 499–507. [[CrossRef](#)]
27. Genova, V.; Paglia, L.; Pulci, G.; Bartuli, C.; Marra, F. Diffusion aluminide coatings for hot corrosion and oxidation protection of nickel-based superalloys: Effect of fluoride-based activator salts. *Coatings* **2021**, *11*, 412. [[CrossRef](#)]

28. Tarel'nyk, V.B.; Gaponova, O.P.; Loboda, V.B.; Konoplyanchenko, E.V.; Martsinkovskii, V.S.; Semirnenko, Y.I.; Tarel'nyk, N.V.; Mikulina, M.A.; Sarzhanov, B.A. Improving ecological safety when forming wear-resistant coatings on the surfaces of rotation body parts of 12Kh18N10T steel using a combined technology based on electrospark alloying. *Surf. Eng. Appl. Electrochem.* **2021**, *57*, 173–184. [[CrossRef](#)]
29. Chinha, A.R. Metallurgical aspects of steels designed to resist abrasion, and impact-abrasion wear. *Mater. Sci. Technol.* **2019**, *35*, 1133–1148. [[CrossRef](#)]
30. Vencel, A.; Vucetic, F.; Bobic, B.; Pitel, J.; Bobic, I. Tribological characterisation in dry sliding conditions of compocasted hybrid A356/SiCp/Grp composites with graphite macroparticles. *Int. J. Adv. Manuf. Technol.* **2019**, *100*, 2135–2146. [[CrossRef](#)]
31. Hovorun, T.; Khaniukov, K.; Varakin, V.; Pererva, V.; Vorobiov, S.; Burlaka, A.; Khvostenko, R. Improvement of the physical and mechanical properties of the cutting tool by applying wear-resistant coatings based on Ti, Al, Si, and N. *J. Eng. Sci.* **2021**, *8*, C13–C23. [[CrossRef](#)]